Functional Plasticity of the Human Humerus: Shape, Rigidity, and Muscular Entheses

Pere Ibáñez-Gimeno,[1] Soledad De Esteban-Trivigno,[2,3] Xavier Jordana,[2] Joan Manyosa,[4] Assumpció Malgosa,[1] and Ignasi Galtés[5,6]*

[1]*Unitat d'Antropologia Biològica, Departament de Biologia Animal, Biologia Vegetal i Ecologia, Universitat Autònoma de Barcelona, 08193 Bellaterra, Barcelona, Catalonia, Spain*
[2]*Institut Català de Paleontologia Miquel Crusafont (ICP), Universitat Autònoma de Barcelona, 08193 Bellaterra, Barcelona, Catalonia, Spain*
[3]*Transmitting Science, Gardenia 2, Can Claramunt, 08784 Piera, Barcelona, Catalonia, Spain*
[4]*Unitat de Biofísica, Departament de Bioquímica i de Biologia Molecular, and Centre d'Estudis en Biofísica, Universitat Autònoma de Barcelona, 08193 Bellaterra, Barcelona, Catalonia, Spain*
[5]*Centre de Patologia Forense de Collserola, Institut de Medicina Legal de Catalunya, Carretera N-150, Km 1.5, 08110 Montcada i Reixach, Barcelona, Catalonia, Spain*
[6]*Unitat de Medicina Legal i Forense, Departament de Psiquiatria i de Medicina Legal, Universitat Autònoma de Barcelona, 08193 Bellaterra, Barcelona, Catalonia, Spain*

KEY WORDS entheseal changes; cross-sectional properties; geometric morphometrics; musculoskeletal stress markers; humerus

ABSTRACT The relationship between the mechanical loading undergone by a bone and its form has been widely assumed as a premise in studies aiming to reconstruct behavioral patterns from skeletal remains. Nevertheless, this relationship is complex due to the existence of many factors affecting bone structure and form, and further research combining structural and shape characteristics is needed. Using two-block PLS, which is a test to analyze the covariance between two sets of variables, we aim to investigate the relationship between upper-limb entheseal changes, cross-sectional properties, and contour shape of the humeral diaphysis. Our results show that individuals with strongly marked entheseal changes have increased diaphyseal rigidities. Bending rigidities are mainly related to entheseal changes of muscles that cross the shoulder. Moreover, the entheseal changes of muscles that participate in the rotation of the arm are related to mediolaterally flatter and ventrodorsally broader humeral shapes in the mid-proximal diaphysis. In turn, this diaphyseal shape is related to diaphyseal rigidity, especially to bending loadings. The shape of the diaphysis of the rest of the humerus does not covary either with rigidity or with entheseal changes. The results indicate that large muscular scars, such as those found in the mid-proximal diaphyses, seem to be related to diaphyseal shape, whereas this relationship is not seen for areas with less direct influences of powerful muscles. Am J Phys Anthropol 000:000–000, 2013.

The concept "mechanical morphogenesis" emphasizes the role of mechanical stimuli in cell division, cell differentiation, and tissue form regulation (Benjamin and Hillen, 2003). In the field of Physical Anthropology, a relationship between mechanical stimuli and bone form has been widely assumed as a premise in studies aiming to reconstruct past behavioral patterns from skeletal material (Ruff, 2000, 2005; Ruff et al., 2006; Meyer et al., 2011). Methodological approaches in the bioarchaeological context have expanded greatly over the last decades with the use of several analytical techniques, such as the study of activity markers (Ruff, 2000; Villotte et al., 2010; Niinimäki, 2012). These are changes in internal and external bone architecture caused by a continued and prolonged stress derived from regular and occupational activities (Kennedy, 1989; Dutour, 1992). Several types of activity markers can be distinguished, including entheseal changes, cross-sectional bone properties, and shape changes (Galtés et al., 2007; Meyer et al., 2011).

Entheseal changes are skeletal markers with a multifactorial causality that are commonly considered to result from an adaptation to muscular loadings (Galtés et al., 2006, 2007; Villotte et al., 2010; Niinimäki and Baiges Sotos, 2012). Diaphyseal cross-sectional properties, which are based on a beam model, reflect the capacity of long bones to resist breaking and deformation (Huiskes, 1982; Ruff, 2008). Bone shape studies are commonly based on external measurements to obtain

Grant sponsor: Ministerio de Ciencia e Innovación; Grant number: CGL2008-00800/BOS; Grant sponsor: Generalitat de Catalunya; Grant number: 2009 SGR 566; Grant sponsor: Programa de Formación de Profesorado Universitario, Ministerio de Educación, Cultura y Deporte; Grant number: AP2009-5102 (P. I-G.); Grant sponsor: Programa Juan de la Cierva, Ministerio de Economía y Competitividad; Grant number: JCI-2010-08157 (X. J.).

*Correspondence to: Ignasi Galtés, Address: Unitat de Medicina Legal i Forense, Departament de Psiquiatria i de Medicina Legal, Universitat Autònoma de Barcelona, 08193 Bellaterra, Barcelona, Catalonia, Spain. E-mail: ignasigaltes@gmail.com

Received 18 July 2012; revised 28 December 2012; accepted 7 January 2013

DOI: 10.1002/ajpa.22234
Published online 00 Month 2013 in Wiley Online Library (wileyonlinelibrary.com).

diaphyseal indices that are assumed to reflect the activity of the individual (Ruff, 2008; Meyer et al., 2011).

There are several areas in the study of skeletal markers of activity that deserve further research, such as their relationship with the biomechanical properties of the bones (Ruff, 2000). There is evidence that the primary response of long bones to changes in mechanical loading is carried out through alterations in diaphyseal geometry and structure (Woo et al., 1981). Nevertheless, while considerable anthropological literature assumes a direct relationship between bone form and mechanical stimuli, there are also studies demonstrating a multifactorial and complex causation (Ruff, 2000; Weiss, 2003; Daly et al., 2004; Niinimäki, 2012). Combining different analysis of bone mechanical response would be useful to obtain a further understanding on their functional significance (Ruff, 2000).

The humerus has been widely used to reconstruct past behavioral patterns. Nevertheless, the functional role of upper-limb muscular activity patterns on humeral diaphyseal shape has only been studied from a descriptive point of view (Rhodes and Knüsel, 2005; Ogilvie and Hilton, 2011). Using a multifactorial approach, the current study aims to investigate the relationship between muscular development, humeral rigidity and diaphyseal shape. Specifically, we aim to determine which specific muscles have the greatest effect on both humeral rigidity and diaphyseal shape.

MATERIALS AND METHODS

Sample

The sample consisted of 62 complete upper-limb specimens (humerus, ulna and radius) of human skeletons housed at the *Unitat d'Antropologia Biològica, Universitat Autònoma de Barcelona* (UAB) (Table 1). These skeletons belong to a contemporary osteological collection of known age and sex (UAB Collection) and to a number of archaeological sites of small communities from all the historical periods. All of them come from populations integrated by rural and manual laborers from Catalonia and Balearic Islands. The age and sex of the latter were estimated by a multifactorial approach according to the criteria proposed by Buikstra and Ubelaker (1994).

Sub-adult individuals were excluded from the study as the appearance and development of their entheses is conditioned by bone immaturity (Hawkey and Merbs, 1995). Although architectural changes occur mostly during growth and entheseal development emerges during adulthood (Hawkey and Merbs, 1995; Rhodes and Knüsel, 2005), mechanical loading can still trigger significant bone architectural responses after adolescence (Ruff et al., 2006). Moreover, entheseal changes are less affected by age in young and mature adults (Galtés et al., 2006). Therefore, only young and mature adults (20–59 years old) were included in the sample. Excluding individuals above 60 years of age, we avoided the most extreme effects of age-related bone loss (Ruff, 2005).

Only the best preserved extremity of each individual was included in the study, and the sample contains right and left specimens in similar proportions. Some individuals were not suitable for all measurements, and so the sample size varies from analysis to analysis. Individuals exhibiting pathological conditions that might affect the musculoskeletal system, such as diffuse idiopathic skeletal hyperostosis (DISH), arthritis or fractures (Aufderheide and Rodríguez-Martín, 1998; Campillo, 2001; Isidro and Malgosa, 2003), were not included in the sample.

TABLE 1. Historical period and age of the studied individuals

	Age		
Historical period	Young adults (20–39)	Mature adults (40–59)	Total
Ancient History and Late Antiquity	13 M 1 F	1 F	15
Middle Ages	10 M 2 F	4 M	16
Early Modern Period	10 M	4 M	14
Contemporary Period	5 M 5 F	5 M 2 F	17
Total	46	16	62

M: males. F: females.

Upper-limb entheseal changes

Eleven upper-limb muscular attachment sites were analyzed on dry bone using the scoring method described by Galtés et al. (2006) and Galtís and Malgosa (2007) (Table 2). This method enables the development of the entheses to be graded according to their morphology, and so both tendinous and direct entheses can be scored (Testut and Latarjet, 1990). Entheses were graded from least to most heavily marked: 0 (no expression), 1 (faint expression), 2 (moderate expression), 3 (strong expression). Entheses with a pathological change, corresponding to grade 4, i.e., presence of ossification exostosis and/or a lytic cortical lesion, were disregarded because they can be caused by factors unrelated to repetitive activity (Ippolito, 1986; Hawkey and Merbs, 1995; Józsa and Józsa, 1997; Galtés et al., 2006; Ibáñez-Gimeno et al., 2012a). Table 3 shows the description of each entheseal development grade for both tendinous and direct entheses. All the entheses analyzed in the current study are tendinous.

In order to evaluate the reproducibility of the method, interobserver and intraobserver errors of the entheseal

TABLE 2. Muscular attachment sites

Muscle	Abbreviation	Analyzed attachment site
Subscapularis	SBS	Lesser tubercle of the humerus
Supraspinatus	SPS	Anteroproximal facet of greater tubercle of the humerus
Infraspinatus	IS	Posteroproximal facet of greater tubercle of the humerus
Teres major	TM	Medial lip of the humeral bicipital groove
Pectoralis major	PM	Lateral lip of the humeral bicipital groove
Deltoid	D	Deltoid tuberosity of the humerus
Extensor digitorum communis	EC	Posterior facet of the humeral lateral epicondyle
Flexor digitorum communis	FC	Anterior facet of the humeral medial epicondyle
Triceps brachii	TB	Posterior surface of olecranon
Brachialis	B	Anterior surface of ulnar coronoid process
Biceps brachii	BB	Bicipital tuberosity of the radius

changes were tested using a total of 330 observations (11 attachment sites of 30 complete upper-limb skeletons). Each specimen was independently assessed by two observers: the main researcher (A) and an external observer (B). Researcher A performed two assessments of the individuals: the first one (A_1) using the 30 individuals; and the second one (A_2), one month later, using a randomized 10% of the total observations. Observer B performed three assessments: the first one (B_1), without previous training, using the 30 individuals and following the descriptions in Table 3; the second one (B_2), one week later, after receiving training and using the 30 individuals; and the third one (B_3), one month later, using the same randomized 10% as observer A. Interobserver error was calculated by comparing A_1 with B_1 and B_2, using the Wilcoxon nonparametric test for two related samples (SPSS 15.0 software, 2006). Intraobserver error was calculated by comparing A_1 with A_2 and B_2 with B_3.

The interobserver comparison test showed significant differences ($P < 0.05$) between A_1 and B_1 for SPS, TM, PM, D, and FC (see Table 2 for the abbreviations). Nevertheless, these differences were not found with the second assessment of the external observer (A_1-B_2). Concerning intraobserver comparison test, identical results were obtained both in A_1-A_2 and B_2-B_3 for all the entheseal changes used in this study.

Geometric morphometrics of the humeral sections

The shape of the humeral diaphysis was assessed by analyzing the outline of diaphyseal cross-sections at different points using geometric morphometrics techniques. NextEngine's 3D Scanner was used to obtain three-dimensional images of the humeri, which were processed with ScanStudio HD software, 2006. The images were exported to the modeling software Rhinoceros 4.0 SR1, 2007, where the longitudinal axis of each humerus was represented as the intersection of coronal and sagittal planes (Ibáñez-Gimeno et al., 2012b). Contours perpendicular to the axis were then obtained at 15, 25, 35, 50 and 75% of bone length (Ruff, 2002) from the distal end. These contours were anatomically oriented using coronal and sagittal planes of the humerus as mediolateral and anteroposterior axes, respectively. Twenty-five semilandmarks were placed all along the outline of each contour (Fig. 1). All semilandmarks were digitized with tpsDig version 1.40, 2004. Each data set (sections at 15, 25, 35, 50 and 75%) was treated separately. Sliding methods may be used to approximate the shape of the curves (Bookstein, 1997; Bookstein et al., 2002; Martinón-Torres et al., 2006; Pérez et al., 2006). Sliding enables semilandmarks to move along the curve. Each semilandmark slides along its tangent to the outline until its final position minimizes one of several possible criteria. The criteria used in the current study is the Procrustes distance between reference and target (Sheets et al., 2004). Sliding was performed using tpdRelW version 1.45, 2007.

The superimposition of all the specimens was performed separately for each dataset (15, 25, 35, 50, and 75%) with MorphoJ 1.04a, 2011, (Klingenberg, 2011) using the Generalized Procrustes Analysis (GPA), which translates, scales and rotates each specimen (semilandmark configuration) in order to minimize Procrustes

TABLE 3. Description of the entheseal development grades for tendinous and direct entheses. Extracted from Galtés et al. (2006)

Grade	Tendinous entheses	Direct entheses
0	The insertion area shows a smooth impression without new bone deposits	The attachment area shows a round or convex surface
1	The insertion area has a visible incipient bone deposit such as granular concretions, fine striations, or a flat and well-defined compact deposit. The rough area is apparent to the touch	The attachment area shows a flattened surface
2	Bone deposit becomes more evident, thick, compacted, elevated, flat-topped.	Development of incipient concavity in the bone surface
3	The defined crust or plaque is uneven. No crests have formed	The attachment area shows a clearly defined concavity

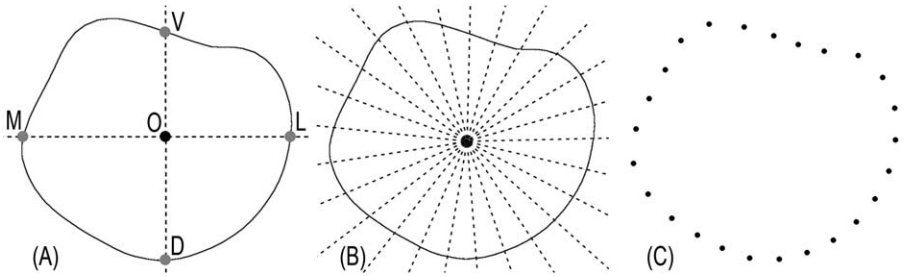

Fig. 1. Placement of semilandmarks in a diaphyseal contour (section at 75% from the distal end of a humerus of the sample is shown as example). The contour is anatomically oriented. **A:** Placement of four points. Points V and D are the intersections between a vertical line that passes through the centroid of the contour (O) and the ventral and dorsal surfaces of the contour, respectively. Points M and L are the intersections between a horizontal line that passes through the centroid of the contour (O) and the medial and lateral surfaces of the contour, respectively. **B:** Circular fan with 25 equiangular lines, drawn with MakeFan 6, 2009. Its center is the central point of the polygon VLDM. **C:** Twenty-five semilandmarks defined as the intersections between each line of the fan and the surface of the contour.

distance between them (Rohlf and Slice, 1990). All specimens were therefore aligned to their mean shape (Zelditch et al., 2004). The results of the generalized Procrustes superimposition are scatters of corresponding semilandmarks (Procrustes shape coordinates) around their means.

Humeral cross-sectional properties

Sections at 35% of humeral length from distal end were used to calculate cross-sectional properties (Ruff, 2008; Sparacello and Marchi, 2008; Nikita et al., 2011). These were assumed to be proper proxies for the characterization of the rigidity, which is defined as the bone capacity to resist deformation, of the entire diaphysis of the humerus (Rhodes and Knüsel, 2005; Ruff, 2008; Niinimäki, 2012). To obtain the sections, the contours at 35% obtained from the three-dimensional images were used as the areas within the sub-periosteal surface. Biplanar radiographs in anteroposterior and mediolateral planes were taken to estimate the contours of the medullary canal (O'Neill and Ruff, 2004; Ruff, 2008).

Scaled images of each cross-section were imported into ImageJ 1.45s, 2011, and analyzed using MomentMacroJ v1.3, 2007. Cortical area (CA) and anatomically oriented second moments of area (I_x, I_y) were calculated for each section. CA is proportional to compression and tension rigidity and I_x and I_y are proportional to antero-posterior and medial-lateral bending rigidities of the bone, respectively (Ruff, 2008). I_x and I_y were standardized by the product of body mass and the second power of bone length, whereas CA was standardized by body mass (Ruff, 2008; Sparacello and Marchi, 2008; Shaw and Stock, 2009a,b). To estimate body mass, femoral anteroposterior head breadth regression formulae were used (Ruff et al., 1991). These body mass estimations are the best approached if the specimens are not from the large or small extremes in size relative to modern humans (Auerbach and Ruff, 2004). Torsional rigidity (J) was not analyzed because it is mathematically dependent on I_x and I_y, and the statistical tests performed in this study require independent variables.

Statistical analyses

Partial Least Squares (PLS) is a wide group of methods for modeling relationships between sets of observed variables by means of latent variables. The underlying assumption of all PLS methods is that the observed data are generated by a system or process driven by a small number of latent (not directly observed or measured) variables (Rosipal and Kramer, 2006). The two-block PLS analysis is a specific PLS method for exploring patterns of covariation between two (although potentially more) blocks of variables which has been widely used in the field of morphometrics over the last few years (see Rohlf and Corti, 2000; Bookstein et al., 2003; McNulty, 2009). The PLS method operates on the covariation between the two blocks of variables, and seeks to obtain a new set of variables that optimally (in the sense of maximal covariance, not correlation) links the blocks using the fewest possible dimensions (McIntosh et al., 1996). The results are pairs of linear combinations that successively maximize the covariance between the sets of variables, while being mutually uncorrelated across sets. Although the PLS and PCA resemble each other in the definition of axes, the former decomposes a matrix into mutually orthogonal axes using the inter-block variance-covariance matrix and the components are ordered according to the amount of covariance between blocks explained by each one, instead of the amount of variance. Moreover, PLS is based on singular value decomposition (SVD), which yields pairs of singular axes, one per block; each pair is associated to a singular value, which is a relative measure of the covariance explained by the paired axes (Zelditch et al., 2004). In this regard, covariance is explained by the singular axis in a manner similar as variance is explained by principal components. Applied to shape data, it identifies those features of shape that have the strongest covariation with the other set of variables. Although both regression and PLS examine the relationship between two sets of variables, they differ in that PLS treat both sets of variables symmetrically, so that it is not implied that the variation in one set of variables is caused by the other set.

The two-block PLS analysis in the context of morphometrics has been mainly used to explore patterns of covariation between shape and other variables, including traditional morphometrics, biomechanical and ecological factors, or behavioral features (Klingenberg and Ekau, 1996; Rohlf and Corti, 2000; Rüber and Adams, 2001; Marugán-Lobón and Buscalioni, 2006); or between two shapes, mainly to address integration and modularity (Bastir and Rosas, 2005; Mitteroecker and Bookstein, 2007).

In order to find out if mechanical loadings derived from muscular activity affect humeral rigidity, the covariance between all entheseal changes and cross-sectional properties was determined by applying a two-block PLS analysis. This analysis also enabled us to determine which muscles have the greatest influence on humeral capacity to resist deformation, since the singular axis corresponding to the non-shape variables can be interpreted using the loadings of the variables on it, in the same way that the loadings in a principal component enable the meaning of that component to be understood. To assess how mechanical loadings derived from muscular activity covary with humeral shape, two-block PLS analyses between each Procrustes coordinates dataset (15, 25, 35, 50 and 75%) and selected entheseal changes for each section were performed. Only entheseal changes of muscles around the studied area were included for the analysis of each section. Two-block PLS analyses between each Procrustes coordinates dataset and cross-sectional properties were also performed with the aim of determining if different humeral rigidities are related to specific diaphyseal shapes. The singular axis corresponding to the block containing shape variables can be depicted graphically by the deformation of the shape configuration along an axis, enabling the interpretation of its biological meaning (Zelditch et al., 2004). Each PLS analysis was performed by pooling within age (young and mature) and sex, so that the differences in the group means were removed. This analysis focuses on the covariation between the deviations from the group averages in the two blocks of variables. Accordingly, the analysis will first remove the differences in the group means, and then the PLS analysis will be run. In order to compute pooled within-group variances and covariances, the deviations of the observations from the group averages of the variables, instead of the deviations from the grand mean, are used. This method makes a correction by subtracting the differences between the group means. The analyses are therefore based on the pooled within-group variation (Klingenberg et al., 2003;

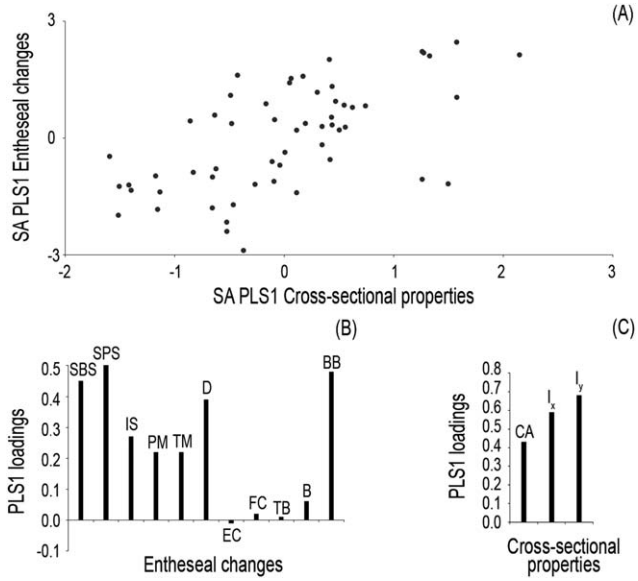

Fig. 2. **A**: Scatterplot of the first extracted singular axes for cross-sectional properties and entheseal changes, resulting from the PLS analysis between these two blocks of variables. These singular axes explain 96.09% of total covariance. Horizontal axis: singular axis (SA) for the block corresponding to cross-sectional properties. Vertical axis: singular axis (SA) for the block corresponding to entheseal changes. **B:** Loadings for each variable of the block corresponding to entheseal changes. See Table 2 for the entheseal changes abbreviations. **C:** Loadings for each variable of the block corresponding to cross-sectional properties.

Klingenberg, 2009). The statistical significance of each PLS analysis was tested with a permutation test of 10000 randomization rounds. All PLS analyses were performed using MorphoJ 1.04a, 2011 (Klingenberg, 2011).

Not all cross-sectional properties used in this study have the same units. Therefore, before running the PLS analyses, these variables were standardized using their *z*-scores. No standardization of the entheseal changes was needed, because their assessment was based on a scale that is equivalent for all the muscles.

Since PLS analyses cannot handle missing data, entheseal changes unobservable or with a pathological change (41 of 682 total observations) were replaced using the median, which is the measure commonly used to replace missing data of ordinal variables (Robb, 1998). For each individual, the median value of his entheseal changes was used to replace the missing data.

RESULTS

The PLS analysis between entheseal changes and cross-sectional properties revealed a statistically significant relationship between them ($N = 56$; RV coefficient = 0.22; $P < 0.001$). A scatterplot of the first singular axes for both blocks of variables is shown in Figure 2A. The loadings of the variables (Fig. 2B,C) indicate that the major relationship between blocks of variables occurs between bending rigidity and the entheseal changes of supraspinatus, biceps brachii, subscapularis, deltoid, infraspinatus, pectoralis major and teres major, in contrast to brachialis, triceps brachii, flexor digitorum communis, and extensor digitorum communis, with loadings close to zero.

TABLE 4. PLS analyses between the shape of each section and selected entheseal changes

Section	Selected entheseal changes	*N*	RV coefficient	*P*
15%	EC, FC, TB, B, BB	58	0.05	0.68
25%	EC, FC, TB, B, BB	62	0.04	0.87
35%	D, TB, B, BB	61	0.06	0.49
50%	PM, D, TB, B, BB	62	0.10	0.07
75%	TM, PM, D, TB, BB	62	0.18	<0.001

The results of PLS analyses between each shape dataset and selected entheseal changes are shown in Table 4. Diaphyseal shape shows significant covariance with entheseal changes of muscles around the corresponding section only at 75% of bone length from the distal end. The first singular axes reveal that more marked entheseal changes of deltoid, pectoralis major and teres major are related to more ventrolaterally developed, laterally narrower and dorsally thicker diaphyses (Fig. 3A,B).

Table 5 shows the results of PLS analyses between each shape dataset and humeral cross-sectional properties. These properties covary with diaphyseal shape at 75% of bone length from the distal end. Ventrodorsally broader diaphyses at 75% are principally related to increased bending rigidities (Fig. 4A,B).

DISCUSSION

Relationship between entheseal changes and diaphyseal rigidity

The results indicate that individuals with strongly marked insertions have increased diaphyseal rigidity, defined as the capacity of the bone to resist deformation (Ruff, 2008). The covariance between both groups of variables is low, which suggests a multifactorial causality of diaphyseal rigidity, as observed in previous studies (Daly et al., 2004; Ruff, 2008; Niinimäki, 2012). According to our results, bending rigidities are mainly related to supraspinatus, biceps brachii, subscapularis, deltoid, infraspinatus, pectoralis major, and teres major. All these muscles cross the shoulder and are involved in its motion (Kapandji, 2002). Conversely, the muscles that do not covary with rigidity, i.e., extensor digitorum communis, brachialis and flexor digitorum communis, cross the elbow but not the mid-distal humerus. In the case of triceps brachii, which does not covary with rigidity either, its long head does cross the shoulder, but its medial and lateral heads do not. These findings are in agreement with the fact that muscles involved in the motion of the shoulder entail complex patterns combining rotation, flexion, extension, abduction and adduction of the arm, thus causing significant bending loading on the humeral shaft (Kapandji, 2002; Escamilla and Andrews, 2009; Gopura et al., 2010).

Previous studies found a relationship between the development of the enthesis of the deltoid and humeral torsion (Carretero et al., 1997), as well as a correlation between humeral robusticity, represented by a composite of several cross-sectional properties, and aggregated entheseal changes of seven major arm muscles (Weiss, 2003). Moreover, a recent analysis indicated the existence of covariation between torsional rigidity and pectoralis major, teres major and deltoid entheses (Niinimäki, 2012). The current study shows that overall muscular development of the arm covaries with humeral

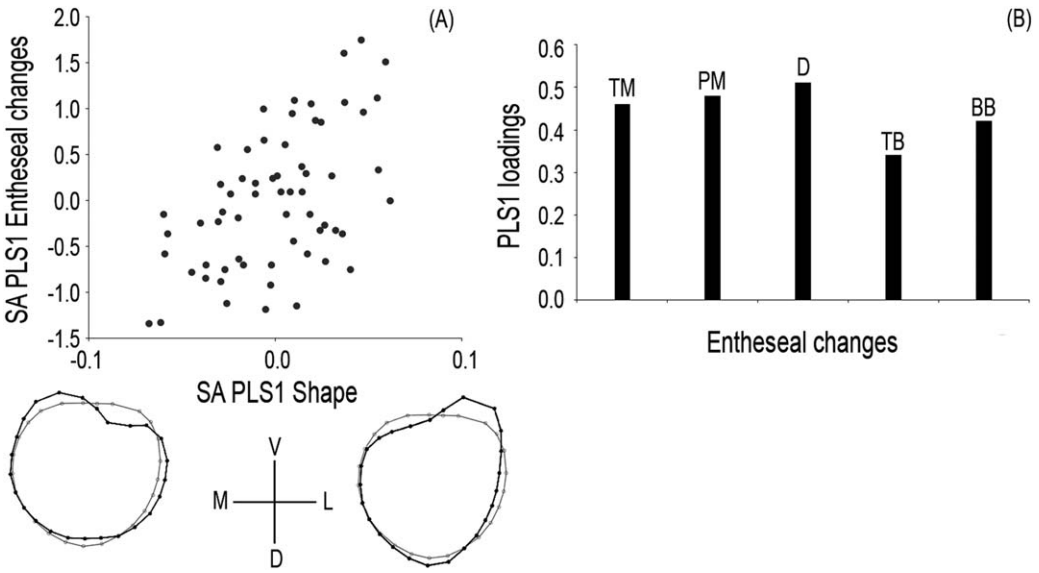

Fig. 3. **A**: Scatterplot of the first extracted singular axes for shape of section at 75% and entheseal changes, resulting from the PLS analysis between these two blocks of variables. These singular axes explain 83.32% of total covariance. Horizontal axis: singular axis (SA) for the block corresponding to shape at 75%; the semilandmark configurations corresponding to the extremes of the singular axis for shape (dark lines and points) are plotted against consensus configuration (in gray) and oriented as indicated. Vertical axis: singular axis (SA) for the block corresponding to entheseal changes. **B:** Loadings for each variable of the block corresponding to entheseal changes. See Table 2 for the entheseal changes abbreviations.

TABLE 5. PLS analyses between shape of each section and cross-sectional properties (CA, I_x, I_y)

Section	*N*	RV coefficient	*P*
15%	56	0.08	0.06
25%	60	0.07	0.08
35%	60	0.06	0.19
50%	60	0.03	0.45
75%	60	0.09	<0.05

rigidity in response to several kinds of loadings, and emphasizes the fact that most relevant covariance occurs between muscles involved in shoulder motion and bending rigidity. The covariance between mid-distal humeral rigidity and entheseal development of shoulder muscles suggests that this region may be used to assess the overall level of proximal upper-limb mechanical loading.

Relationship between entheseal changes and diaphyseal shape

According to our results, mechanical loadings derived from muscular activity covary with diaphyseal shape only at 75% of humeral length (mid-proximal diaphysis). This may be related to the fact that a number of powerful muscles attach onto the diaphysis around this area (pectoralis major, teres major, latissimus dorsi, deltoid, coracobrachialis, and triceps brachii), whereas in the remaining sections muscular attachment sites are not that numerous. Of all these muscles, the highest covariation is found for deltoid, pectoralis major and teres major muscles. Mechanical loadings derived from the activity of these muscles lead to mediolaterally flatter and ventrodorsally broader humeral shapes. The existence of a relationship between pectoralis major and deltoid muscles and ventrodorsally diaphyseal broadening had been previously suggested by Rhodes and Knüsel (2005). The implication of teres major in this covariation is also possible, because all these muscles are involved in the same muscular chain (Kapandji, 2002; Escamilla and Andrews, 2009). The ability of these muscles to perform rotational movements depends, not only on their muscular power, but also on the distances between muscular insertion sites and the rotational axis of the arm, which explains the observed ventrodorsally broader shapes at 75% of humeral length. Therefore, the loadings derived from the activity of these muscles lead to a mid-proximal diaphysis with this shape.

Mechanical loading derived from activity was indicated to be the main cause of entheseal development when using the scoring method applied here (Galtés et al., 2006). Nevertheless, the multifactorial etiology of the entheseal changes (Benjamin et al., 2002; Alves Cardoso and Henderson, 2010; Villotte et al., 2010; Villotte and Knüsel, 2012) could be partially influencing the lack of relationship found between entheseal changes and shape at 15, 25, 35, and 50%. In any case, the lack of covariance in the mid-distal diaphysis suggests that general robusticity, rather than shape, may be the most meaningful characteristic to assess in this region. Shape at 35% of humeral length is difficult to interpret (Ruff and Larsen, 2001; Rhodes and Knüsel, 2005; Sparacello and Marchi, 2008), and so shape measures should not be limited to this section (Trinkaus et al., 1994). In any case, functional inferences from long bone cross-sectional shape should be made with caution (Demes et al., 2001; Ruff et al., 2006).

Relationship between diaphyseal rigidity and diaphyseal shape

The results indicate that humeral rigidity covaries with diaphyseal shape only at 75% of bone length.

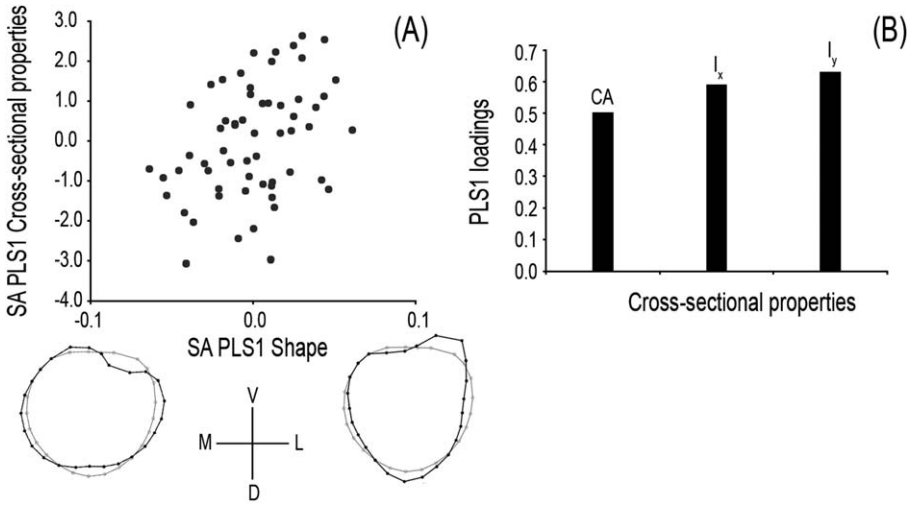

Fig. 4. **A**: Scatterplot of the first extracted singular axes for shape of section at 75% and cross-sectional properties, resulting from the PLS analysis between these two blocks of variables. These singular axes explain 94.53% of total covariance. Horizontal axis: singular axis (SA) for the block corresponding to shape at 75%; the semilandmark configurations corresponding to the extremes of the singular axis for shape (dark lines and points) are plotted against consensus configuration (in gray) and oriented as indicated. Vertical axis: singular axis (SA) for the block corresponding to cross-sectional properties. **B:** Loadings for each variable of the block corresponding to cross-sectional properties.

Ventrodorsally broader and mediolaterally flatter diaphyses in this area are related to increased rigidities, especially bending rigidities. Shape changes at 75% associated to increased rigidities are clearly related to insertions of the more proximal muscles, i.e., pectoralis major, teres major, and deltoid, which may influence muscular loadings of the humeral shaft as a whole (Niinimäki, 2012). This is confirmed by the abovementioned reported covariance between entheseal changes of muscles that cross the shoulder and bending rigidity.

Therefore, in the proximal humerus, shape changes reflecting muscular development, i.e., insertion sites and adjacent areas, are related to mechanical loads, and thus to cross-sectional properties. Cross-sectional properties do not covary with the shape of the rest of the sections. At 15 and 25%, the tendons of the flexor and extensor digitorum communis create ridges on the medial and lateral sides of the diaphysis, respectively. Nevertheless, the mechanical loading derived from these muscles is not as relevant as that from the shoulder muscles, and the results fail to find covariance in this region. At 35% and 50%, shape does not covary with cross-sectional properties either, which is consistent with the fact that there are no large muscle scars in these areas (Aiello and Dean, 1990). Although the section at 50% may include the distal end of the deltoid tuberosity, the major part of the enthesis is more proximal. The shape in these areas, therefore, is less influenced by the mechanical loading derived from muscular activity, which is in agreement with the lack of covariance between entheseal changes and shape at 15, 25, 35, and 50% of humeral length. The beam model theory is dependent on nonabrupt changes in morphology or loadings, since abrupt changes create stress concentrations and invalidate the model (Huiskes, 1982; Daegling, 2002). Therefore, our findings support the general consensus on choosing 35 or 50% regions to characterize humeral rigidity (Bridges et al., 2000; Maggiano et al., 2008; Ruff, 2008; Nikita et al., 2011; Ogilvie and Hilton, 2011).

Classical anthropological studies reconstruct behavioral patterns from mid-distal and mid-shaft diaphyseal indices of the humerus (robusticity and diaphyseal index) (Olivier, 1960; Bass, 1971). The results of the current study indicate that mid-proximal shape of the humerus is more affected by activity than the rest of the humeral diaphysis. Therefore, this area should be considered and analyzed when aiming to reconstruct activity patterns from skeletal remains.

CONCLUSIONS

This study provides evidence to support the generalized assumption of the existence of a relationship between the shape of the humeral diaphysis, its rigidity and the upper-limb entheseal changes, although other parameters, such as hormonal levels, genetic precursors, bone density and other aspects, could be influencing this relationship in some measure. The activity patterns of the studied individuals were decomposed in the entheseal changes of the eleven muscles analyzed in this paper, and so the mechanical loadings derived from these muscles, rather than the activity patterns, were used to determine the covariance between the studied sets of variables, reducing the effect that the inclusion of different populations in the sample may have on the outcomes. Humeri with greater rigidities present more developed entheseal changes of those muscles that cross the shoulder. Moreover, the entheseal changes of the muscles that participate in the rotation of the arm are more developed in those individuals that have a mid-proximal humeral diaphysis with a ventrodorsally broad shape, which in turn have greater diaphyseal rigidities. This indicates that the mid-proximal diaphysis may be used to assess the overall level of proximal upper-limb mechanical loading. Nevertheless, the shape of the diaphysis of the rest of the humerus does not covary either with rigidity or with entheseal changes. Large muscular scars, such as those found in the mid-proximal

diaphyses, seem to be related to diaphyseal shape, whereas this relationship is not seen for areas with less direct influences of powerful muscles, e.g., changes in diaphyseal morphology caused by local insertions.

ACKNOWLEDGMENTS

The authors thank Núria Armentano, Susana Carrascal and Eulàlia Subirà for providing part of the studied sample. They are grateful to Rut Cañas, Dominika Nociarová and Elena Fiorin for their assistance during the analysis of the sample. They are also thankful to Christopher B. Ruff and two anonymous reviewers for their comments and suggestions on an earlier version of this manuscript.

LITERATURE CITED

Aiello LC, Dean C. 1990. An introduction to human evolutionary anatomy. East Kilbride: Academic Press.

Alves Cardoso F, Henderson CY. 2010. Enthesopathy formation in the humerus: data from known age-at-death and known occupation skeletal collections. Am J Phys Anthropol 141:550–560.

Auerbach BM, Ruff CB. 2004. Human body mass estimation: a comparison of "morphometric" and "mechanical" methods. Am J Phys Anthropol 125:331–342.

Aufderheide AC, Rodríguez-Martín C. 1998. The Cambridge Encyclopedia of human paleopathology. Cambridge: Cambridge University Press.

Bass WM. 1971. Human osteology: a laboratory and field manual of the human skeleton. Columbia: Missouri Archaeological Society.

Bastir M, Rosas A. 2005. Hierarhical nature of morphological integration and modularity in the human posterior face. Am J Phys Anthropol 128:26–34.

Benjamin M, Hillen B. 2003. Mechanical influences on cells, tissues and organs: 'Mechanical morphogenesis'. Eur J Morphol 41:3–7.

Benjamin M, Kumai T, Milz S, Boszczyk BM, Boszczyk AA, Ralphs JR. 2002. The skeletal attachment of tendons: tendon 'entheses'. Comp Biochem Phys A 133: 931–945.

Bookstein FL, Gunz P, Mitteroecker P, Prossinger H, Schaefer K, Seidler H. 2003. Cranial integration in *Homo*: singular warps analysis of the midsagittal plane in ontogeny and evolution. J Hum Evol 44:167–187.

Bookstein FL, Sampson PD, Connor PD, Streissguth AP. 2002. Midline corpus callosum is a neuroanatomical focus of fetal alcohol damage. Anat Rec B 269:162–174.

Bookstein FL. 1997. Landmark methods for forms without landmarks: morphometrics of group differences in outline shape. Med Image Analysis 1:225–243.

Bridges PS, Blitz JH, Solano MC. 2000. Changes in long bone diaphyseal strength with horticultural intensification in west-central Illinois. Am J Phys Anthropol 112:217–238.

Buikstra JE, Ubelaker DH, editors. 1994. Standards for data collection from human skeletal remains. Fayetteville: Arkansas Archeological Society.

Campillo D. 2001. Introducción a la paleopatología. Barcelona: Edicions Bellaterra.

Carretero JM, Arsuaga JL, Lorenzo C. 1997. Clavicles, scapulae and humeri from the Sima de los Huesos site (Sierra de Atapuerca, Spain). J Hum Evol 33:357–408.

Daegling DJ. 2002. Estimation of torsional rigidity in primate long bones. J Hum Evol 43:229–239.

Daly RM, Saxon L, Tumer CH, Robling AG, Bass SL. 2004. The relationship between muscle size and bone geometry during growth and in response to exercise. Bone 34:281–287.

Demes B, Qin Y-X, Stern JT, Larson SG, Rubin CT. 2001. Patterns of strain in the macaque tibia during functional activity. Am J Phys Anthropol 116:257–265.

Dutour O. 1992. Activités physiques et squelette humain: Le difficile passage de l'actuel au fossile. B Mem Soc Anthropol Par 4:233–241.

Escamilla RF, Andrews JR. 2009. Shoulder muscle recruitment patterns and related biomechanics during upper extremity sports. Sports Med 39:569–590.

Galtés I, Jordana X, García C, Malgosa A. 2007. Marcadores de actividad en restos óseos. Cuadernos de Medicina Forense 48-49:179–189.

Galtés I, Malgosa A. 2007. Atlas metodológico para el estudio de marcadores musculoesquelético de actividad en el radio. Paleopatología 3. Available at: http://www.ucm.es/info/aep/paleopatologia/vol3/radiomini.pdf.

Galtés I, Rodríguez-Baeza A, Malgosa A. 2006. Mechanical morphogenesis: a concept applied to the surface of the radius. Anat Rec A 288A:794–805.

Gopura RARC, Kiguchi K, Horikawa E. 2010. A study on human upper-limb muscles activities during daily upper-limb motions. Int J Bioelectromagn 12:54–61.

Hawkey DE, Merbs CF. 1995. Activity-induced musculoskeletal stress markers (MSM) and subsistence strategy changes among ancient Hudson Bay Eskimos. Int J Osteoarchaeol 5:324–338.

Huiskes R. 1982. On the modeling of long bones in structural-analyses. J Biomech 15:65–69.

Ibáñez-Gimeno P, Galtés I, Jordana X, Fiorin E, Manyosa J, Malgosa A. 2012a. Entheseal changes and functional implications of the humeral medial epicondyle. Int J Osteoarchaeol. DOI: 10.1002/oa.2299.

Ibáñez-Gimeno P, Jordana X, Manyosa J, Malgosa A, Galtés I. 2012b. 3D analysis of the forearm rotational efficiency variation in humans. Anat Rec 295:1092–1100.

ImageJ 1.45s. 2011. Public domain software for Windows. Bethesda: Wayne Rasband, National Institutes of Health, USA.

Ippolito E. 1986. Insertional tendinopathies, stenosing tenosynovitis, exudative hypertrophic tenosynovitis, peritendinitis, and tendinosis and metaplasia. In: Perugia L, Postacchini F, Ippolito E, editors. The tendons. Milano: Editrice Curtis. p 113–213.

Isidro A, Malgosa A, editors. 2003. Paleopatología. La enfermedad no escrita. Masso: Barcelona.

Józsa L, Józsa PK. 1997. Human tendons: anatomy, physiology, and pathology. Champaign, IL: Human Kinetics.

Kapandji AI. 2002. Fisiología articular, miembro superior. Madrid: Editorial Médica Panamericana.

Kennedy KAR. 1989. Skeletal markers of occupational stress. In: Iscan MY, Kennedy KAR, editors. Reconstruction of life from the skeleton. New York: Alan R. Liss, Inc. p 129–160.

Klingenberg CP, Ekau W. 1996. A combined morphometric and phylogenetic analysis of an ecomorphological trend: pelagization in Antarctic fishes (Perciformes: Nototheniidae). Biol J Linn Soc 59:143–177.

Klingenberg CP, Mebus K, Auffrayc J-C. 2003. Developmental integration in a complex morphological structure: how distinct are the modules in the mouse mandible? Evol Dev 5:522–531.

Klingenberg CP. 2009. Morphometric integration and modularity in configurations of landmarks: tools for evaluating *a priori* hypotheses. Evol Dev 11:405–421.

Klingenberg CP. 2011. MorphoJ: an integrated software package for geometric morphometrics. Mol Ecol Resour 11:353–357.

Maggiano IS, Schultz M, Kierdorf H, Sosa TS, Maggiano CM, Blos VT. 2008. Cross-sectional analysis of long bones, occupational activities and long-distance trade of the Classic Maya from Xcambo': archaeological and osteological evidence. Am J Phys Anthropol 136:470–477.

MakeFan 6. 2009. Software for Windows. Integrated Morphometrics Package. Buffalo: Canisius College.

Martinón-Torres M, Bastir M, De Castro JMB, Gomez A, Sarmiento S, Muela A, Arsuaga JL. 2006. Hominin lower second premolar morphology: evolutionary inferences through geometric morphometric analysis. J Hum Evol 50:523–533.

Marugán-Lobón J, Buscalioni AD. 2006. Avian skull morphological evolution: exploring exo- and endocranial covariation with two-block partial least squares. Zoology 109:217–230.

McIntosh AR, Bookstein FL, Haxby JV, Grady CL. 1996. Spatial pattern analysis of functional brain images using partial least squares. NeuroImage 3:143–157.

McNulty KP. 2009. Computing singular warps from Procrustes aligned coordinates. J Hum Evol 57:191–194.

Meyer C, Nicklisch N, Held P, Fritsch B, Alt KW. 2011. Tracing patterns of activity in the human skeleton: an overview of methods, problems, and limits of interpretation. Homo 62:202–217.

Mitteroecker P, Bookstein FL. 2007. The conceptual and statistical relationship between modularity and morphological integration. Syst Biol 56:818–836.

MomentMacroJ v1.3. 2007. ImageJ plugin, software for Windows. Baltimore: Christopher Ruff, Center for Functional Anatomy and Evolution. Available at: http://www.hopkinsmedicine.org/fae/mmacro.htm.

MorphoJ 1.04a. 2011. Software for Windows. Manchester: Klingenberg lab, The University of Manchester.

Niinimäki S. 2012. The relationship between musculoskeletal stress markers and biomechanical properties of the humeral diaphysis. Am J Phys Anthropol 147:618–628.

Niinimäki S, Baiges Sotos L. 2012. The relationship between intensity of physical activity and entheseal changes on the lower limb. Int J Osteoarchaeol. DOI: 10.1002/oa.2295.

Nikita E, Ysi Siew Y, Stock J, Mattingly D, Lahr MM. 2011. Activity patterns in the Sahara Desert: an interpretation based on cross-sectional geometric properties. Am J Phys Anthropol 146:423–434.

Ogilvie MD, Hilton CE. 2011. Cross-sectional geometry in the humeri of foragers and farmers from the Prehispanic American southwest: exploring patterns in the sexual division of labor. Am J Phys Anthropol 144:11–21.

Olivier G. 1960. Pratique anthropologique. Paris: Vigot Frères Eds.

O'Neill MC, Ruff CB. 2004. Estimating human long bone cross-sectional geometric properties: a comparison of noninvasive methods. J Hum Evol 47:221–235.

Pérez SI, Bernal V, González PN. 2006. Differences between sliding semi-landmark methods in geometric morphometrics, with an application to human craniofacial and dental variation. J Anat 208:769–784.

Rhinoceros 4.0 SR1. 2007. Educational edition for Windows. Seattle: Robert McNeel & Associates.

Rhodes JA, Knüsel CJ. 2005. Activity-related skeletal change in medieval humeri: cross-sectional and architectural alterations. Am J Phys Anthropol 128:536–546.

Robb JE. 1998. The interpretation of skeletal muscle sites: a statistical approach. Int J Osteoarchaeol 8:363–377.

Rohlf FJ, Corti M. 2000. Use of two-block partial least-squares to study covariation in shape. Syst Biol 49:740–753.

Rohlf FJ, Slice D. 1990. Extensions of the Procrustes method for the optimal superimposition of landmarks. Syst Zool 39:40–59.

Rosipal R, Krämer N. 2006. Overview and recent advances in partial least squares. In: Saunders C, Grobelnik M, Gunn S, Shawe-Taylor J, editors. Subspace, latent structure and feature selection techniques. Berlin: Springer. p 34–51.

Rüber L, Adams DC. 2001. Evolutionary convergence of body shape and trophic morphology in cichlids from Lake Tanganyika. J Evolution Biol 14:325–332.

Ruff CB, Holt B, Trinkaus E. 2006. Who's afraid of the big bad wolff? "Wolff's law" and bone functional adaptation. Am J Phys Anthropol 129:484–498.

Ruff CB, Scott WW, Liu AYC. 1991. Articular and diaphyseal remodeling of the proximal femur with changes in body-mass in adults. Am J Phys Anthropol 86:397–413.

Ruff CB. 2000. Biomechanical analyses of archaeological human skeletons. In: Katzenberg MA, Saunders SR, editors. Biological anthropology of the human skeleton. New York: Wiley-Liss. p 71–102.

Ruff CB. 2002. Long bone articular and diaphyseal structure in Old World monkeys and apes. I. locomotor effects. Am J Phys Anthropol 119:305–342.

Ruff CB. 2005. Mechanical determinants of bone form: insights from skeletal remains. J Musculoskelet Neuronal Interact 5:202–212.

Ruff CB. 2008. Biomechanical analyses of archaeological human skeletons. In: Katzenberg MA, Saunders SR, editors. Biological anthropology of the human skeleton, 2nd ed. New York: Wiley-Liss. p 183–206.

Ruff CB, Larsen CS. 2001. Reconstructing behavior in Spanish Florida: the biomechanical evidence. In: Larsen CS, editor. Bioarchaeology of Spanish Florida: the impact of colonialism. Gainesville: University Press of Florida. p 113–145.

ScanStudio HD 1.2.1. 2006. Software for Windows. Santa Monica: NextEngine.

Shaw CN, Stock JT. 2009a. Habitual throwing and swimming correspond with upper limb diaphyseal strength and shape in modern human athletes. Am J Phys Anthropol 140:160–172.

Shaw CN, Stock JT. 2009b. Intensity, repetitiveness, and directionality of habitual adolescent mobility patterns influence the tibial diaphysis morphology of athletes. Am J Phys Anthropol 140:149–159.

Sheets DH, Kim K, Mitchel CE. 2004. A combined landmark and outline-based approach to ontogenetic shape change in the Ordovician Trilobite *Triarthrus becki*. In: Elewa A, editor. Morphometrics: applications in biology and paleontology. Berlin: Springer-Verlag. p 67–82.

Sparacello V, Marchi D. 2008. Mobility and subsistence economy: a diachronic comparison between two groups settled in the same geographical area (Liguria, Italy). Am J Phys Anthropol 136:485–495.

SPSS 15.0. 2006. Software for Windows. Chicago: SPSS Inc.

Testut L, Latarjet A. 1990. Tratado de anatomía humana. Barcelona: Salvat Editores.

tpdRelW version 1.45. 2007. Software for Windows. Brookhaven: James Rohlf, SUNY at Stony Brook.

tpsDig version 1.40. 2004. Software for Windows. Brookhaven: James Rohlf, SUNY at Stony Brook.

Trinkaus E, Churchill SE, Ruff CB. 1994. Postcranial robusticity in Homo. II: humeral bilateral asymmetry and bone plasticity. Am J Phys Anthropol 93:1–34.

Villotte S, Castex D, Couallier V, Dutour O, Knüsel CJ, Henry-Gambier D. 2010. Enthesopathies as occupational stress markers: evidence from the upper limb. Am J Phys Anthropol 142:224–234.

Villotte S, Knüsel CJ. 2012. Understanding entheseal changes: definition and life course changes. Int J Osteoarchaeol. DOI: 10.1002/oa.2289.

Weiss E. 2003. Understanding muscle markers: aggregation and construct validity. Am J Phys Anthropol 121:230–240.

Woo SLY, Kuei SC, Amiel D, Gomez MA, Hayes WC, White FC, Akeson WH. 1981. The effect of prolonged physical-training on the properties of long-one: a study of Wolff's law. J Bone Joint Surg Am 63:780–787.

Zelditch ML, Swiderski DL, Sheets DH, Fink WL. 2004. Geometric morphometrics for biologists: a primer. Boston: Elsevier Academic Press.